

Compact Damping Models for Lateral Structures Including Gas Rarefaction Effects

Timo Veijola

Helsinki University of Technology,
Department of Electrical and Communications Engineering,
Circuit Theory Laboratory, P.O.Box 3000, FIN-02015 HUT, Finland,
E-mail:timo@aplac.hut.fi, Tel: +358-9-4512293, Fax: +358-9-4514818.

ABSTRACT

Compact models for the viscous damping coefficient in narrow air gaps between laterally moving structures are reported. The gas rarefaction effects are included in these small-displacement models. In the first part of the paper, a simple frequency-independent first-order slip-flow approximation for the damping coefficient is derived. The resulting simple approximation has a maximum relative error of less than $\pm 0.6\%$ at arbitrary Knudsen numbers at viscous, transitional and free molecular regions.

In the second part of the paper, the dynamic model for the damping force is derived, considering again the gas rarefaction, by applying the slip-velocity boundary conditions. An analytic expression for the damping coefficient to be used in the frequency-domain analysis of an oscillating structure is presented. These dynamic model is implemented also as an electrical equivalent admittance, constructed of RC sections, to allow both frequency and time domain simulations with a circuit simulator.

Keywords: Gas damping, Effective viscosity, Knudsen number, Rarefied Couette flow, Damping in microstructures

1 INTRODUCTION

The internal friction of the gas, the viscosity, in the gaps between moving structures generates forces proportional to velocity, that is, damping forces. At low pressures or at very narrow gaps, typical for micromechanical devices, the behaviour of the gas flow will change due to the gas rarefaction effect. The damping mechanism for structures that move perpendicular to their surfaces is called squeezed-film damping effect. In [1], simple approximations for the rarefaction effect in this squeezed-film damping case have been presented in the form of an effective viscosity.

When the structures move in parallel with their surfaces, e.g., in various surface-micromachined structures, the flow velocity profile is quite different: linear (Couette flow) instead of parabolic (Poiseuille flow). The squeezed-film effective viscosity equations do not apply in this case. Moreover, the damping phenomena

at high surface velocities are not restricted to narrow gaps. The dissipation also takes place at the “boundary layer”, that will be formed close to the moving surface.

In the first part of this paper, two models for the gas rarefaction effect for surfaces moving slowly ($Re \ll 1$) in parallel with the surfaces are compared: the first-order slip-flow approximation [2] and a more accurate model derived from the linearized Boltzmann equation by several authors, e.g., Cercignani and Pagani [3] and Shakhov [4]. As a result of the comparison, the first-order model is slightly adjusted to decrease its relative maximum error from about 7% to $\pm 0.6\%$.

The second part of this paper discusses the damping at higher velocities ($Re \geq 1$), that is, the frequency-dependency of the damping is included in the model. At a relatively high frequency, the inertia of the gas will change considerably the flow profile, effectively increasing the damping. Zhang and Tang [5] have given a model for the frequency dependency by using a simple formula for the penetration depth. Cho et al. [6] have given a more complicated model for the frequency dependent damping coefficient. In this paper, these models are extended to include the gas rarefaction effects. Since the slip-flow boundary conditions give good results at low velocities, they are also applied to approximate the solution at higher velocities.

First, an analytic expression is derived that models the damping force of an oscillating plate as a function of frequency. Then, a general dynamic model, valid in both the frequency and the time domain, is implemented approximately as an electrical equivalent circuit.

2 FREQUENCY-INDEPENDENT DAMPING MODEL

Assume two surfaces bounding a flat gas film. The first surface, at $z = d$ moves with velocity v_r in the direction of the x axis, while the second at $z = 0$ does not move, see Fig. 1. The surfaces are assumed large compared with other dimensions, and thus the border effects are ignored here.

2.1 First-order Slip-velocity Model

At low surface velocities ($Re \ll 1$), the gas velocity profile can be assumed to be linear, and due to the gas

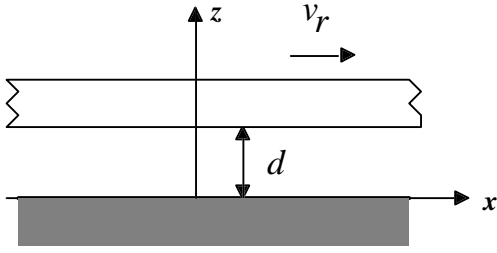


Figure 1: Structure of the air-gap.

rarefaction, the gap width effectively increases by 2λ , where λ is the mean free path of the gas. According to Burgdorfer [2], the shear stress at one of the surfaces is

$$\tau_{xz} = \frac{\eta A}{d + 2\lambda} v_r, \quad (1)$$

where A is the surface area and η is the viscosity coefficient. The contribution of the mean free path can be included into the effective viscosity:

$$\eta_{\text{eff},s} = \frac{\eta}{1 + 2K_n}, \quad (2)$$

where K_n , the Knudsen number, is the measure of the rarefaction effect. It is the ratio between the mean free path λ and gap height d : $K_n = \lambda/d$. The resulting damping coefficient ξ is then simply

$$\xi = \frac{\tau_{xz}}{v_r} = \frac{\eta_{\text{eff},s} A}{d}. \quad (3)$$

2.2 Kinetic Gas Model

In order to find a more accurate model for the effective viscosity, the linearized Boltzmann equation is applied instead of the slip velocity boundary conditions. Cercignani and Pagani [3] presented an analytic solution to this problem with variational methods. They expressed the stress τ_{xz} relative to the stress in the free molecular region $\tau_{xz,\text{fm}}$:

$$\tau_{xz} = \pi_{xz} \tau_{xz,\text{fm}}, \quad (4)$$

where

$$\pi_{xz} = \frac{1}{2} + T_1(D) + \frac{\sqrt{\pi}}{2} J_{\text{min}}, \quad (5)$$

where $D = \sqrt{\pi}/(2K_n)$ is the inverse Knudsen number, J_{min} is the minimum value of a functional, and functions $T_n(x)$ are the Abramowitz functions [7]. Using a linear trial function, the expression for J_{min} is [3] (the equations in the original reference contain printing errors)

$$J_{\text{min}} = -\frac{c_1^2}{c_{11}}, \quad (6)$$

where

$$c_1 = \frac{1}{\sqrt{\pi}} \{ D[1 + 2T_1(D)] + 4T_2(D) - \sqrt{\pi} \},$$

$$c_{11} = \frac{1}{\sqrt{\pi}} \{ D^2[1 + 2T_1(D)] + 8DT_2(D) + 8T_3(D) - 4 \}.$$

For large D , π_{xz} approaches $\sqrt{\pi}/D$ (this result has been confirmed more numerically than analytically).

When D approaches infinity, $\eta_{\text{eff},b}$ approaches η , and we can write

$$\eta_{\text{eff},b} = \frac{\pi_{xz} D}{\sqrt{\pi}} \eta. \quad (7)$$

The damping effect due to the gas rarefaction is smaller than in the squeezed-film damping case, but even at atmospheric pressures in air ($\lambda = 64$ nm) and in a $1 \mu\text{m}$ gap, the effective viscosity decreases the damping coefficient of about 12%. Since the mean free path is inversely proportional to the pressure, the damping will be considerably smaller at lower pressures.

The slip-flow equation (2) differs from Eq. (7) mostly at around $K_n = 1$. Its maximum relative deviation is about 7%, and the error approaches 0 at small and large values of K_n .

2.3 Improved Slip-Flow Approximation

For practical implementation in computer programs or for hand-calculus, a modified expression for Eq. (7) is given here. The modified expression, a result of curve fitting, for the effective viscosity is

$$\eta_{\text{eff},m} = \frac{\eta}{1 + 2K_n + 0.2 \cdot K_n^{0.788} e^{-K_n/10}}. \quad (8)$$

The maximum relative error of this approximation, at all values of K_n , is less than $\pm 0.6\%$

3 DYNAMIC DAMPING MODEL

The model presented in the previous section of this paper assumes a full established Couette flow ignoring the inertia effect of the gas. To extend the damping model to be valid at higher frequencies, the time-dependent velocity profile of the gas must be considered. The dynamics of the gas is modelled with the one-dimensional diffusion equation

$$\frac{\partial v(z)}{\partial t} = \nu \frac{\partial^2 v(z)}{\partial z^2}, \quad (9)$$

where ν is the kinematic viscosity $\nu = \eta/\rho$ and ρ is the density of the gas.

3.1 Frequency-Domain Analytic Model

Eq. (9) can be solved in the frequency-domain for a steady-state sinusoidal velocity excitation having an amplitude of v_r . The boundary conditions for the velocity $v(z)$ including the slip velocity are [2]

$$v(0) = v_r + \lambda \left. \frac{\partial v(z)}{\partial z} \right|_{z=0}, \quad (10)$$

$$v(d) = -\lambda \left. \frac{\partial v(z)}{\partial z} \right|_{z=d}. \quad (11)$$

The velocity function that satisfies Eq. (9) with the given boundary conditions is

$$v(z) = -v_r \frac{\sinh(qd - qz) + q\lambda \cosh(qd - qz)}{(1 + q^2\lambda^2) \sinh(qd) + 2q\lambda \cosh(qd)}, \quad (12)$$

where $q = \sqrt{j\omega/\nu}$ is the complex frequency variable. The shear stress acting on a surface of area A is

$$\bar{\tau}_{xz} = -\eta A v_r \left. \frac{\partial v(z)}{\partial z} \right|_{z=0}. \quad (13)$$

Substituting Eq. (12) in Eq. (13) yields

$$\bar{\xi} = \frac{\bar{\tau}_{xz}}{v_r} = \eta A q \frac{\cosh(qd) + q\lambda \sinh(qd)}{(1 + q^2\lambda^2) \sinh(qd) + 2q\lambda \cosh(qd)}. \quad (14)$$

The damping coefficient is the real part of $\bar{\xi}$ and the imaginary part of $\bar{\xi}$ can be interpreted as the contribution of an additional effective mass sticking to the surface. The damping coefficient is

$$\text{Re}(\bar{\xi}) = \eta A \beta \frac{\sinh(2\beta d) + \sin(2\beta d) + k_1}{\cosh(2\beta d) - \cos(2\beta d) + k_2}, \quad (15)$$

where $\beta = \sqrt{\omega/(2\nu)}$ and

$$\begin{aligned} k_1 &= 4\gamma[(1 + \gamma^2) \cosh(2\beta d) + (1 - \gamma^2) \cos(2\beta d)] \\ &\quad + 6\gamma^2[\sinh(2\beta d) - \sin(2\beta d)], \\ k_2 &= 4\gamma[(1 + 2\gamma^2) \sinh(2\beta d) + (1 - 2\gamma^2) \sin(2\beta d)] \\ &\quad + 4\gamma^2[(2 + \gamma^2) \cosh(2\beta d) + (2 - \gamma^2) \cos(2\beta d)], \end{aligned}$$

where $\gamma = \beta\lambda$.

Let us analyze the properties of Eq. (14) in a few extreme cases. When $\lambda = 0$, $k_1 = k_2 = 0$ and Eq. (15) reduces to the expression given by Cho et al. [6], and when ω approaches 0, it approaches the frequency-independent damping coefficient given in Eq. (3). Moreover, when ω approaches infinity, the damping coefficient will approach a real value of $\eta A/\lambda$. This indicates that a ‘‘boundary layer’’ of width λ has been established.

The accuracy can be improved, at least at low frequencies, by applying the model derived from the Boltzmann equation in Eq. (8). This is accomplished simply by multiplying the damping coefficient by $\eta_{\text{eff,m}}/\eta_{\text{eff,s}}$.

3.2 Electrical Equivalent Circuit Model

For frequency domain analysis, the admittance in Eq. (14) can be implemented as a single circuit element whose value is directly evaluated at each frequency point. A model that is valid in both the time and the frequency domain can be implemented as an electrical equivalent circuit applying electrical equivalencies: velocity is interpreted as voltage and force is interpreted as current, whereas the damping coefficient is equivalent to an electrical admittance.

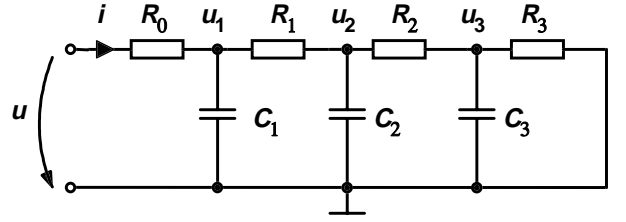


Figure 2: Electrical equivalent circuit that realizes the damping admittance. A circuit with 3 section is shown.

The admittance can be approximately synthesized with a ladder circuit consisting of RC sections, as shown in Fig. 2. Each section models the flow admittance of a small slice of the gas between $z = r_n$ and $z = r_{n+1}$. The node voltages u_n between the sections represent the flow velocity at discrete distances $z = r_n$.

The value of the first resistance $R_0 = \lambda/\eta/A$ ensures that the admittance approach the correct asymptotic value at high frequencies. The remaining resistance values are

$$R_n = \frac{1 - \lambda/d}{\eta A} (r_{n+1} - r_n), \quad n = 1, 2, \dots, N. \quad (16)$$

The values for the capacitors are

$$C_n = \begin{cases} \rho A r_{1.5}, & n = 1, \\ \rho A (r_{n+0.5} - r_{n-0.5}), & n = 2, 3, \dots, N-1, \\ \rho A (d - r_{N-0.5}), & n = N. \end{cases} \quad (17)$$

When $r_1 = 0$ and $r_{N+1} = d$, the low frequency conductance is accurately modelled. The distances r_n and the number of sections may be freely selected, depending on the accuracy desired. In practice, radii synthesized using an increasing geometric series give good results.

This electrical-equivalent model has been included in the library of microelectromechanical components written for the circuit simulation program APLAC [8], [9].

4 MODEL VERIFICATION

A laterally oscillating plate of $1 \text{ mm} \times 1 \text{ mm}$ at various gap heights is studied. The air pressure is 1 atm. The contribution of the gas rarefaction to the shear force is first demonstrated. Figure 3 shows the coefficient $\bar{\xi}$ given by Eq. (14) as a function of frequency with and without the gas rarefaction effect.

Figure 4 compares the admittances given by the analytic equation with the admittance of the equivalent circuit at various gap heights. Four sections are used in the equivalent circuit.

A transient response of the equivalent circuit model for a sinusoidal velocity excitation at 500 MHz (amplitude is 1 mm/s) is performed. The resulting shear force is shown in Fig. 5 for three gap heights.

5 CONCLUSIONS

Both an analytic frequency domain model and an electrical equivalent circuit model for estimating the shear stress due to the rare gas in laterally moving structures were given. The first-order slip-flow boundary conditions resulted in a good low frequency model (relative error $< 7\%$), and the accuracy was further improved using kinetic gas theory (relative error $< 0.6\%$).

The same boundary conditions were applied also to derive a model for relatively large frequencies. However, the validity of these slip-flow conditions has not been verified for $K_n \gg 1$, and the actual error of the model is not known. Measurements or a solution using the linearized Boltzmann equation [10] could reveal the error of the approximation. Moreover, in practical structures, the finite length and width of the structure will increase the damping, as shown by Zhang and Tang [5].

REFERENCES

- [1] T. Veijola, H. Kuisma, and J. Lahdenperä, "The influence of gas-surface interaction on gas film damping in a silicon accelerometer," *Sensors and Actuators A*, vol. 66, pp. 83–92, 1998.
- [2] A. Burgdorfer, "The influence of the molecular mean free path on the performance of hydrodynamic gas lubricated bearings," *Journal of Basic Engineering, Trans. ASME*, vol. 81, pp. 94–99, Mar. 1959.
- [3] C. Cercignani and C. D. Pagani, "Variational approach to boundary-value problems in kinetic theory," *The Physics of Fluids*, vol. 9, pp. 1167–1173, June 1966.
- [4] E. M. Shakhov, "Rarefied gas shear flow between two movable segments of parallel plates," *Fluid Dynamics*, vol. 30, no. 3, pp. 462–466, 1995.
- [5] X. Zhang and W. C. Tang, "Viscous air damping in laterally driven microresonators," *Sensors and Materials*, vol. 7, no. 6, pp. 415–430, 1995.
- [6] Y. Cho, A. P. Pisano, and R. T. Howe, "Viscous damping model for laterally oscillating microstructures," *Journal of Microelectromechanical Systems*, vol. 3, pp. 81–87, June 1994.
- [7] M. Abramowitz and I. A. Stegun, *Handbook of Mathematical Functions*. Dover publications, Inc., New York, 1965.
- [8] T. Veijola, H. Kuisma, and J. Lahdenperä, "Dynamic modelling and simulation of microelectromechanical devices with a circuit simulation program," in *MSM'98*, (Santa Clara), pp. 245–250, Apr. 1998.
- [9] <http://www.aplac.hut.fi/aplac>.
- [10] F. Coron, "Derivation of slip boundary conditions for the Navier-Stokes system from the Boltzmann equation," *Journal of Statistical Physics*, vol. 54, no. 3/4, pp. 829–857, 1989.

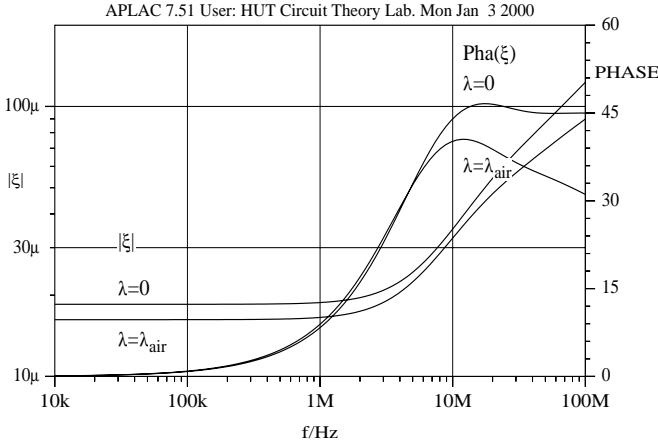


Figure 3: The contribution of the finite mean free path λ to the damping coefficient at atmospheric pressure. Gap separation is $1\ \mu\text{m}$ and the surface area is $1\ \text{mm} \times 1\ \text{mm}$.

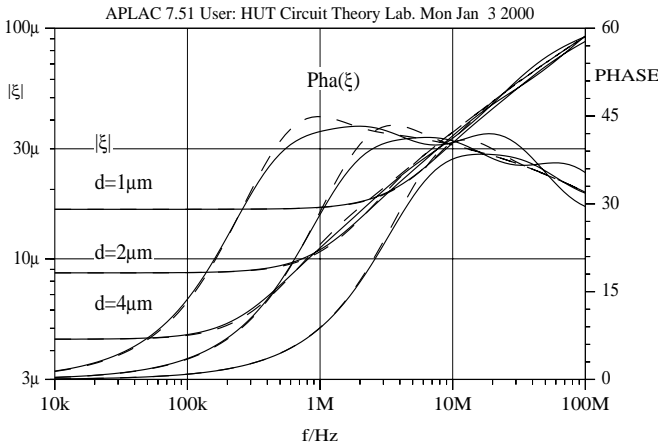


Figure 4: The frequency response of the synthesized admittance (—) compared with the analytic admittance in Eq. (8) (---) at three gap heights.

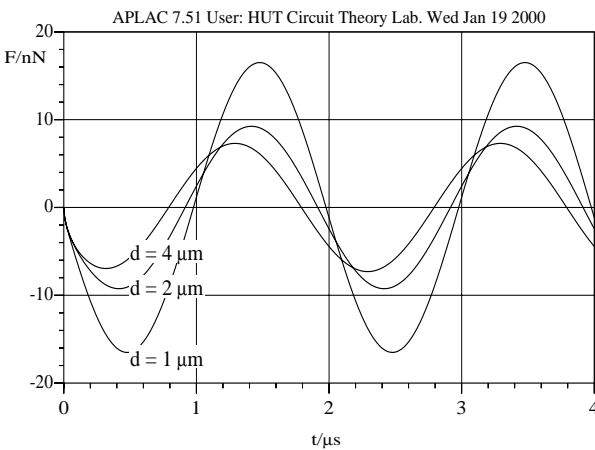


Figure 5: Shear force as a function of time analyzed with the electrical equivalent circuit model.